Article citation info:
FERDYNUS M, KOTEŁKO M, KRAL J. Energy absorption capability numerical analysis of thin-walled prismatic tubes with corner dents under axial impact. Eksploatacja i Niezawodnosc – Maintenance and Reliability 2018; 20 (2): 252–259, http://dx.doi.org/10.17531/ein.2018.2.10.

Mirosław FERDYNUS
Maria KOTEŁKO
Jan KRAL

ENERGY ABSORPTION CAPABILITY NUMERICAL ANALYSIS OF THIN-WALLED PRISMATIC TUBES WITH CORNER DENTS UNDER AXIAL IMPACT

NUMERYCZNA ANALIZA ENERGOCHŁONNOŚCI CIENKOŚCIENNYCH SŁUPÓW PRYZMATYCZNYCH Z PRZETŁOCZENIAMI

The paper presents results of a parametric study into energy absorption capability of thin-walled square section columns with redrawn dents, subjected to axial impact compressive load. Thin-walled aluminum tubes with four dents in the corners were under investigation. The varying parameters were the dent's depth and distance of the dent to the base. The study was performed using Finite Element numerical code. Three crashworthiness indicators were examined: peak crushing force, crash load efficiency and stroke efficiency. The numerical results are shown in load-shortening diagrams, as well as diagrams and maps of crashworthiness indicators. It was found, that the main factor influencing a crushing mode and, subsequently, energy absorption capability, is a dent depth. The dent distance from the base is of less importance. Also a position of a dent, either at the bottom, or at the top base (the load application point) does not influence the crushing behavior significantly. For the deepest dents the relative increase of crash load efficiency (CLE) amounts 25% in comparison with the column without dents.

Keywords**:** *crashworthiness indicators, energy absorber, thin walled member.*

W artykule przedstawiono wyniki badań numerycznych zdolności pochłaniania energii energoabsorberów w postaci cienkościennych słupów o przekroju kwadratowym z wgłębieniami, poddanych osiowym obciążeniom udarowym. Badano wpływ parametrów geometrycznych oraz położenia inicjatorów zgniotu w postaci walcowych przetłoczeń w narożach na zachowanie się konstrukcji oraz właściwości energoabsorbcyjne (współczynnik efektywności zgniotu- Ste oraz procentowy stosunek siły średniej do maksymalnej - CLE). Obliczenia numeryczne prowadzono z wykorzystaniem MES, programu Abaqus 6.14. Wyniki przedstawiono w postaci charakterystyk obciążenie – skrócenie oraz diagramów i wykresów. Stwierdzono, że istotny wpływ na zachowanie się konstrukcji podczas uderzenia oraz jej energochłonność ma głębokość przetłoczenia, mniej istotne jest jego położenie. W przypadku słupów z najgłębszymi przetłoczeniami względny wzrost współczynnika CLE, w porównaniu z wynikami uzyskanymi dla słupa gładkiego wynosi 25%.

Słowa kluczowe*: wskaźniki energoabsorbcyjne, absorber energii, konstrukcje cienkościenne.*

1. Introduction

Increasing number of impacting events of many types like traffic accidents, collisions of ships or collisions of a ship either with an iceberg or ship grounding on a narrow rock, etc. induced the rapid development of the impact crashworthiness dealing with research into impact engineering problems, particularly in the field of dynamic response of structures in the plastic range and the design of energy absorbers. Since demands of general public of the safe design of components of vehicles, ships, etc. have increased substantially in the last few decades, a new challenge appeared to design special structural members which would dissipate the impact energy in order to limit the deceleration and finally to stop a moveable mass (e.g. vehicle) in a controlled manner. Such a structural member termed the energy absorber converts totally or partially the kinetic energy into another form of energy. One of the possible design solutions is the conversion of the kinetic energy of impact into the energy of plastic deformation of a thin-walled metallic structural member.

In the early sixties of the 20th century, automotive safety regulations stimulated the development of the new concept of a crashworthy (safe) vehicle that had to fulfil the integrity and impact energy management requirements [2]. A designer of any impact attenuation device must meet two main, sometimes contrary requirements: The initial collapse load has to be not too high in order to avoid unacceptably high impact deceleration of the vehicle. On the other extreme, the main requirement is a possibly highest energy dissipation capacity, which may not be achieved if the collapse load of the impact device is too low. The latter may result in dangerously high occupant "ridedown" decelerations.

Thus, maximizing energy absorption and minimizing peak to mean force ratio by seeking for the optimal design of these components are of great significance.

There are numerous types of energy absorbers of that kind that are cited in the literature [4,6]. Namely, there are steel drums, thin tubes or multi-corner columns subject to compression, compressed frusta (truncated circular cones), simple struts under compression, sandwich plates or beams (particularly honeycomb cells) and many others. Among all those design solutions, mentioned above, thin-walled metal tubes are widely used as energy absorption systems in automotive industry due to their high energy absorption capability, easy to fabricate, relatively low price and sustainability at collapse.

In the case of thin-walled members subjected to axial compression, which act as energy absorbers, a substantial issue is such a design, which promotes a progressive buckling mechanism, stimulating the highest energy absorption capacity. One of the possible design solutions is the application of a trigger (notch or dent), which releases the most desirable crushing mechanism. There are numerous published results of research concerning energy absorption of thin-walled tubes [2,4,6], however, few deal with tubular structures with dents or other flaws.

2. State of the art: an overview

As was mentioned above, metal tubes, particularly of prismatic cross-section, subjected to impact load, have been investigated since 60-ties of the 20th century [3]. Many efforts have been made so far by several researchers to reduce the peak load at the initial stage of the crushing process and simultaneously to increase energy absorption capacity in such members, acting as energy absorbers [2,6].

At the turn of centuries, a new class of tubular energy absorbers have been introduced, namely axially loaded thin-walled foam-filled metal columns made of different foam material, like polyurethane, metal, polypropylene, etc.. Energy absorbed during the crushing process by such members consists of the energy dissipated in the metal tube and the energy dissipated in the filler.

The problem of the crushing behavior of such members was initially investigated by Hanssen et al. [11,12]. Then, Wang et al. [20] published the results concerning closed-hat section columns filled with aluminum foam. They derived a theoretical model of such columns and developed a constitutive material model of the aluminum foam on the basis of experimental tests.

In last two decades numerous research results concerning the problem of foam-filled metal columns acting as energy absorbers have been published [6]. Because of many parameters influencing energy absorption capability and more and more complex structural design of such members, optimization procedures occurred to be necessary. One of the first attempts in this area were published by Zarei and Kroger [22], who performed the optimization of the foam-filled aluminum tube.

In the first decade of 21th century, multi-cell columns have been introduced as energy absorbers, hollow and foam-filled. Chen and Wierzbicki [7] published theoretical results concerning crushing behavior of such structural members. They investigated the axial crushing of multi-cell hollow columns, using analytical and numerical methods and of double-cell and triple-cell foam-filled columns, using FE method. Very recently, Yin et al. [21] performed multi-objective crashworthiness optimization of foam-filled multi-cell columns using different metamodel techniques. The optimization criteria were maximum energy absorption and minimum peak crushing force. They carried out the multi-objective optimization using four metamodels and stated, that the most effective one was Radial Basis Function (RBF) model.

In last few years, research was carried out into another solution, namely the application of multi-cornered thin-walled tubes as energy absorbing members [6]. Abbasi et al. [1] investigated the crushing behavior and energy absorption of hexagonal, octagonal and 12-edge thin-walled columns. Reddy et al. [18] continued to analyze the similar problem for 12-edge columns of different geometry. Ali et al. [5] analyzed the axial crushing of pentagonal and cross-shape thin-walled tubes. Another solution, bitubal energy absorber was investigated experimentally under quasi-static load by Sharifi et al. [19].

Very recently, W. Liu et al. [17] performed the crashworthiness multi-objective optimization of sandwich star-shaped tubes. They investigated a multi-wall structure, with a star-shaped tube between two circulars.

Another alternative solution are flaws or dents acting as triggers. A trigger may induce the most desirable crushing (collapse) mode, leading to higher energy absorption and mean to peak crushingforce ratio.

Very few published papers deal with tubular structures with dents, dimples or other flaws. An interesting solution has been presented by Z. Yang [23]. The subject of investigation was the crushing behavior of a thin-walled circular tube with internal gradient grooves. The authors fabricated stainless steel thin-walled tube with preset internal circumferential rectangular groove defects using SLM 3D printing method. They observed double buckling-splitting crushing mode. Empty and foam-filled circumferentially grooved thick-walled circular tubes under axial low velocity impact were investigated theoretically and experimentally by A. Darvizeh et al. [8]. In [9] the effect of discontinuity size on the energy absorption performance of square profiles was reported. In [16] the authors studied the behavior of tubular columns with dents, but these flaws were treated as imperfections coming from damage.

One of the first attempts to apply columns with dents as energy absorbers, namely a static analysis of axially compressed square section tube with dents in the corners is presented in [10]. The subject of the investigation was a square-section column with periodically (along the height) situated dimples (redrawn dents) in the corners. FE simulations of crushing behavior were carried out. Very recently, Yang et al [15] investigated circular tubes with periodically situated (both along the circumference and the height) ellipsoidal dimples, subjected to axial crushing force. FE simulations of crushing behavior were performed and experimentally validated by quasi-static tests on 3D printed brass tubes.

The above state of the art overview shows that no research has been undertaken so far into crushing behavior and crashworthiness of thin-walled columns with a prismatic cross-section and non-periodically situated dents. In this paper the crushing behavior of such structural members subjected to axial impact load is investigated.

3. Subject and aim of the investigation

3.1. Structural geometry

The subject of this investigation was a thin-walled square section aluminum tube with four indentations in the corners, formed by means of cylindrical redrawing. The tubes with the dimensions □70x2 and height l=335 mm were investigated.

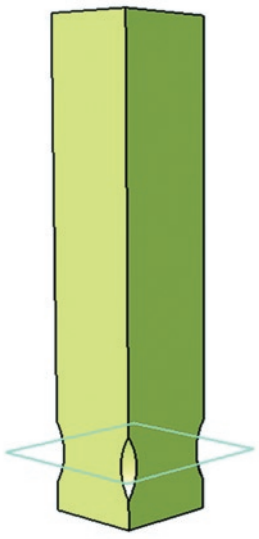

Fig. 1. Column model with dents generated in Catia v5 system

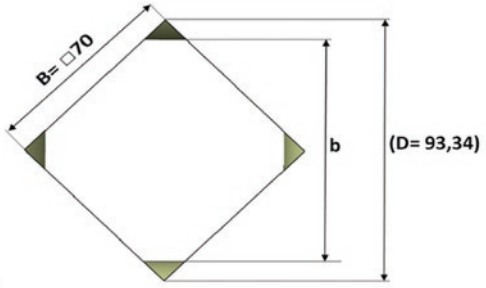

Fig. 2. Cross-section of the column in the mid-surface of the dent (D=93,34 mm)

The process of modeling of the column with dents was realized with the Catia v. 5 software package in the Generative Shape Design module. The geometrical model was exported to the Abaqus code module. The dent's geometry was characterized by the main radius R=50 mm and relative dent depth with respect to the dimension **b** of the main diagonal (Fig.2) in the column's cross-section (from 5% up to 30%). The dents were made at the bottom of the column (Fig.1,3) or at the top (Fig.3). The models with the dents at the bottom of the column were designated by the symbols from A05_X to A30_X, where the first number stands for the relative depth of the dent (in percentage) while X stands for the distance of the dent from the bottom (Fig.4). Similarly, the models with dents situated at the top of the column (where the impact load was applied) were designated by the column symbols C05_X to C30_X, where X was measured from the top of the column. The column with smooth walls (without dents) was denoted as SM.

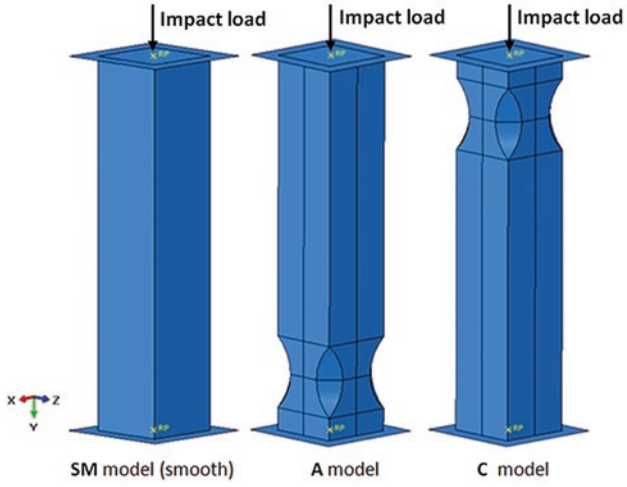

Fig. 3. Investigated column models

A05_X	A10_X	A15_X	A20_X	A25_X	A30_X
b=88.67	b=84.01	b=79.34	b=74.67	b=70.01	b=65.34
X= 5; 10; 15; 20; 25; 30					

Fig. 4. Geometric parameters of A models

4. FE model

Crushing behavior analysis of the investigated columns was performed on the basis of FE simulations. The FE explicit analysis was carried out using Abaqus 6.13 code. The column was situated between two rigid plates (Fig. 3). An FE model of the column was created using 4-node shell elements S4R and it was subjected to impact load of the kinetic energy E= 7.5 kJ, which corresponds to the mass m= 150 kg dropping with the initial velocity V_0= 10 m/s.

The columns were assumed to be made from the aluminum alloy EN AW6060- T6 (σ_Y=175 MPa, σ_{ult}=250 MPa, ν=0.33). Since aluminum alloys do not display a significant sensitivity to the strain rate, a bi-linear material model was applied, neglecting an influence of the strain rate, but taking into account the strain hardening (E=70000MPa, E_t=937,5MPa).

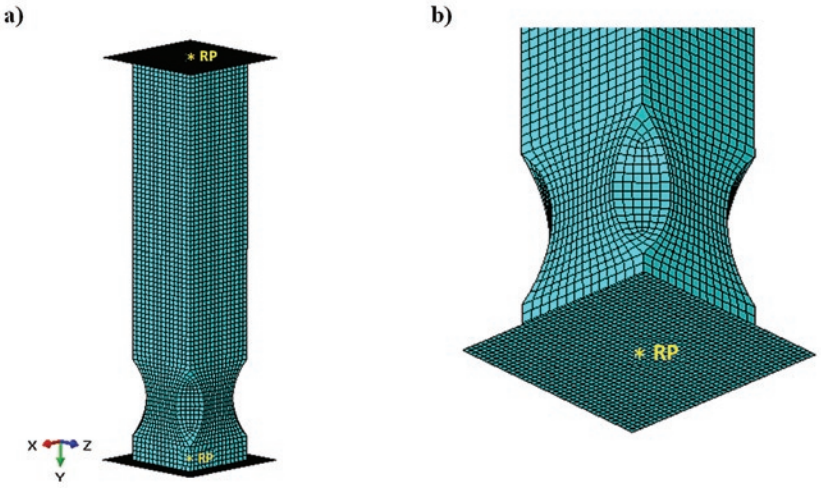

Fig. 5. FE model of the investigated column

In the rigid plates reference points RP were created, where the impact force (at the bottom point) and acceleration, velocity, displacement (at the top point) were recorded. The reference points are shown in Fig. 5. All degrees of freedom were taken (switched off) at the bottom rigid plate, while at the top plate only one degree of freedom, in the axial direction y, was possible.

5. Crushing behaviour

The results of the FE calculations reveal, that the failure mode of the investigated flawed columns depends mainly on the redrawing depth (dent depth). Three following main modes of failure were observed: For the smallest values of the dent depth (A05), regardless of the dent position (X), the crushing process was initiated by the local plastic mechanism (first local fold) situated at the center of the column (Fig.6). Also for A10, but for the position of dent X = 5-15, the same failure mode was observed. For medium values of dents depth (A10, A15) and X≤20 mm, the crushing process was triggered by the local plastic mechanism situated above the dent (Fig.7). For the largest values of dent depths (A20, A25, A30), regardless of the position of the dent, crushing was initiated by a local plastic mechanism situated exactly at the dent. These three types of failure are denoted below as mode I, mode II and mode III, respectively.

The specification of the crushing modes of columns A in terms of dent depth and position of the dent is shown in Table 1.

A preliminary FE study indicated, that the position of the dent, either at the bottom of the column (A) or at the top (C), does not influence the column's structural behavior significantly, which is shown in Fig. 9 and subsequent Fig. 10 and 11. The

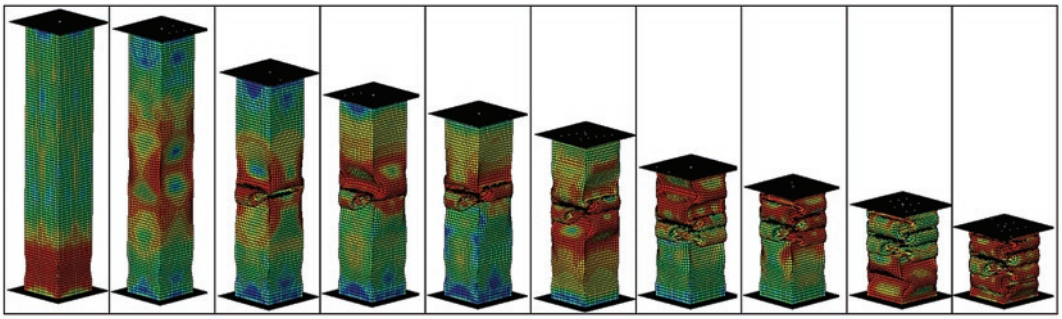

Fig 6. Crushing mode I (column A05_15)

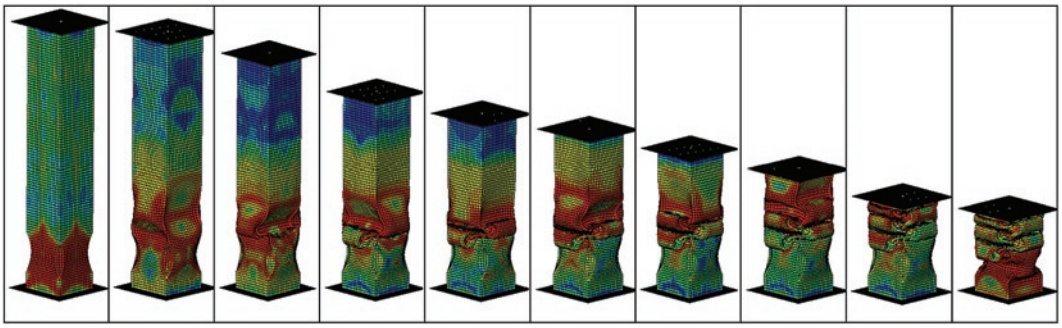

Fig.7. Crushing mode II (column A15_20)

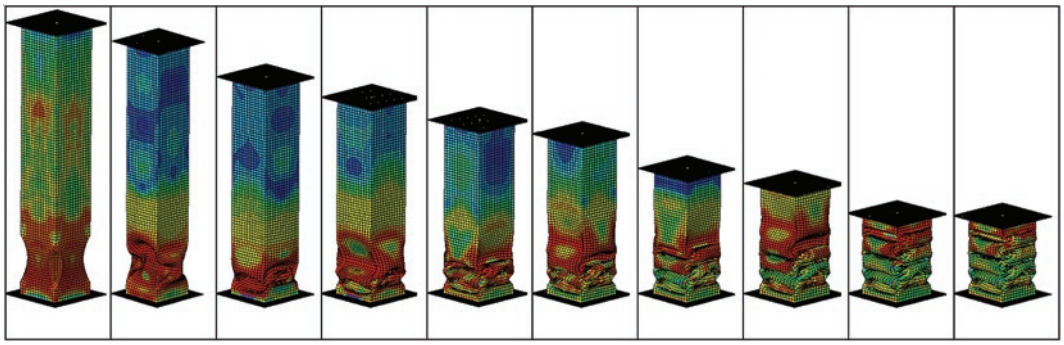

Fig. 8. Crushing mode III (column A20_10)

Table 1. Specification of columns A crushing modes

	Model					
	A05_X	**A10_X**	**A15_X**	**A20_X**	**A25_X**	**A30_X**
X=5	I	I	II	III	III	III
X=10	I	I	II	III	III	III
X=15	I	I	II	III	III	III
X=20	I	II	II	III	III	III
X=25	I	III	III	III	III	III
X=30	I	III	III	III	III	III

only more significant differences were observed with respect to the PCF factor (larger for the C option). Thus, a further detailed parametric study was focused on the column type A.

In all load-shortening diagrams the ordinate indicates the load value RF2 recorded at the lower reference point RP shown in Fig. 5. The abscissa indicates the vertical displacement U2 recorded at the upper reference point RP, also shown in Fig.5.

6. Parametric study

There are several crashworthiness indicators [13,14] used to evaluate the crashworthiness of the energy absorbing structure (energy absorber). In the present analysis, the following indicators are applied: energy absorption (EA), mean crushing force (MCF), crash load efficiency (CLE), stroke efficiency (St_e).

The typical crushing force – displacement curve for a thin-walled member subjected to axial impact is shown in Fig.12.

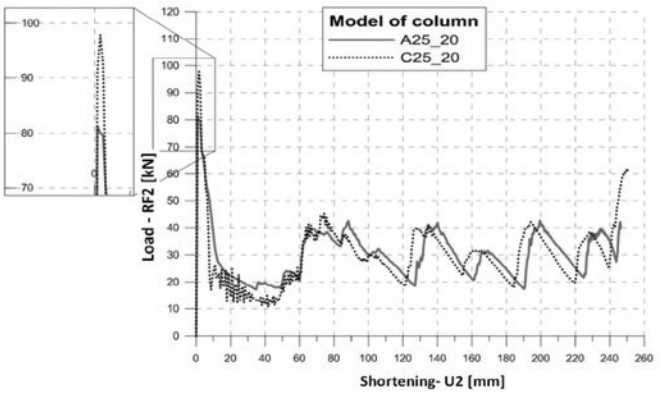

Fig. 9. Comparative load-shortening diagrams of column model A25_20 and C25_20

Table 2. Comparison of crashworthiness indicators for columns A and C

Model	U2max [mm]	PCF [kN]	MCF [kN]	St_e [-]	CLE [%]
SM	228,98	104,469	32,77	0,316	31,37
A25_20	246,27	87,557	30,48	0,265	34,79
C25_20	250,35	97,90	30,01	0,253	30,65

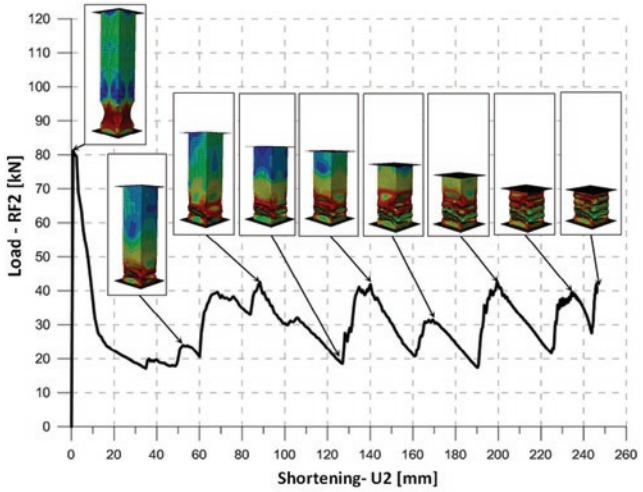

Fig 10. Load-shortening diagram of column model A25_20 (indication of characteristic failure stages)

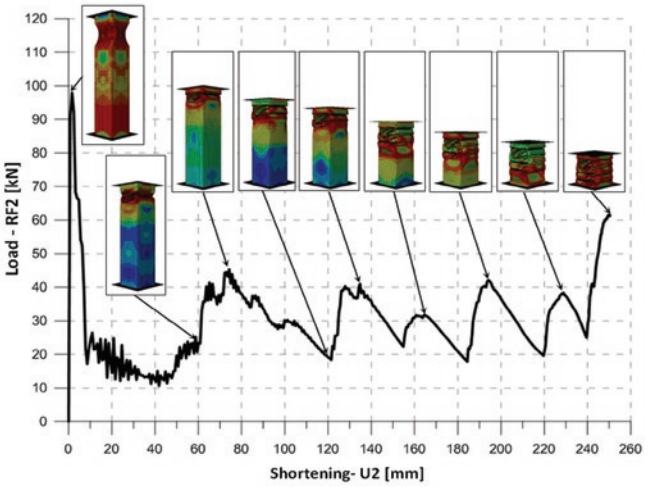

Fig. 11. Load-shortening diagram of column model C25_20 (indication of characteristic failure stages)

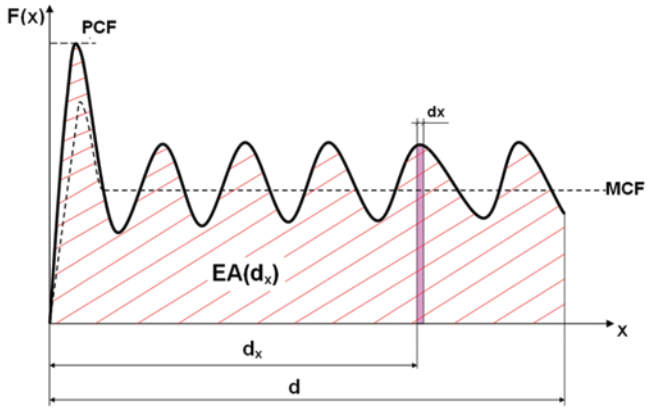

Fig. 12. Exemplary load-shortening diagram of thin-walled column under axial impact

$$EA(d_x) = \int_0^{d_x} F(x)dx \tag{1}$$

where d_x is a crushing distance (see Fig.12).

The mean crushing force (MCF) for a given crushing deformation d_x is calculated as:

$$MCF = \frac{EA(d_x)}{d_x} \tag{2}$$

The crash load efficiency is a mean crushing force (MCF) to peak crushing force (PCF – see Fig.12) ratio:

$$CLE = \frac{MCF}{PCF} \cdot 100\% \tag{3}$$

The stroke efficiency Ste is defined as follows:

$$St_e = \frac{L_o - U}{L_o} \tag{4}$$

where:

L_0 – is the initial length (characteristic dimension) of the member [mm],

U – is the maximum shortening (maximum characteristic deformation) of the member [mm]

A detailed parametric study into an optimal design of depth and position of the dents with respect to the column's energy absorption capability, namely crashworthiness indicators mentioned above (MCF, CLE and St_e), was performed on the basis of the FE simulations results.

As was mentioned above, the preliminary study showed, that the crushing behavior of columns A (bottom dent) and C (top dent) does not differ. Also, the values of crashworthiness indicators for these two types of columns are similar (except PCF), which is presented in Table 2. The difference in the Ste factor amounts to about 4.5%, while the CLE factor is larger about 12% for the A option. Since the A option (trigger at the bottom) is more desirable, the results presented below concern columns type A only.

Fig. 13. shows the load-shortening diagrams for columns A with different dent depths and the same dent position, which exhibited

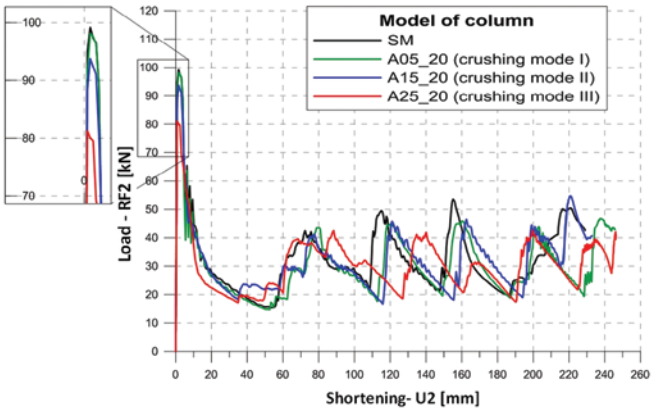

Fig. 13. Load-shortening diagrams for columns A exhibiting three different crushing modes (constant value of X=20 mm)

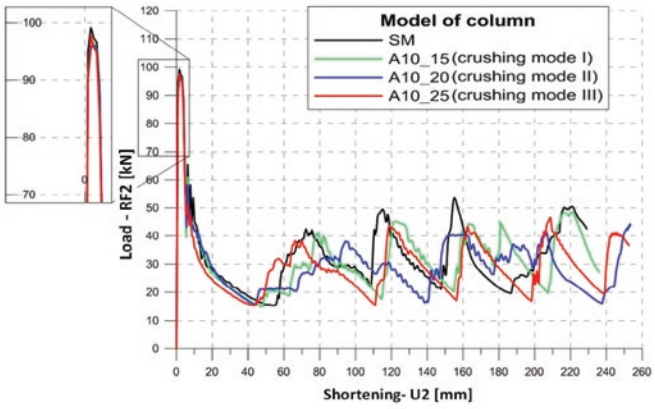

Fig. 14. Load-shortening diagrams for columns A exhibiting three different crushing modes (constant value of relative dent depth = 10%)

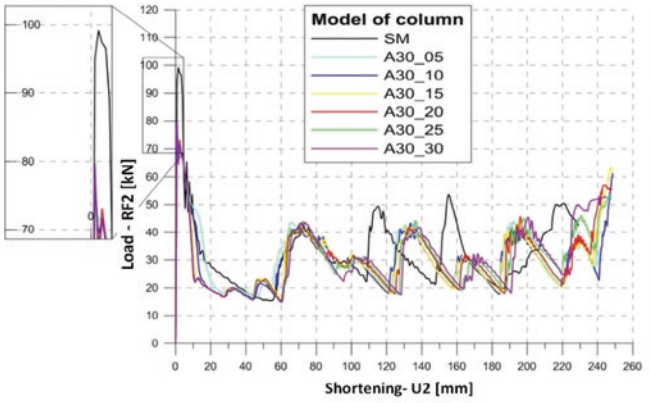

Fig. 15. Load-shortening diagrams for columns A exhibiting crushing mode III (constant value of relative dent depth = 30%)

three different crushing modes (see Table 1). The character of these diagrams is nearly the same. A significant decrease in the peak crushing force (PCF) is observed in comparison with the column without dents (SM). For the columns A10 (with the relative dent depth of 10%) also three crushing modes were observed, depending on the dent situtation X. Comparative load-shortening diagrams for three columns A10 of three X positions corresponding to three crushing modes are presented in Fig. 14. Also in that case the character of three diagrams is the same. In „blow-up" piece of the diagram one can notice, that PCF depends mainly on redrawing depth and, in minor extent, on X position.

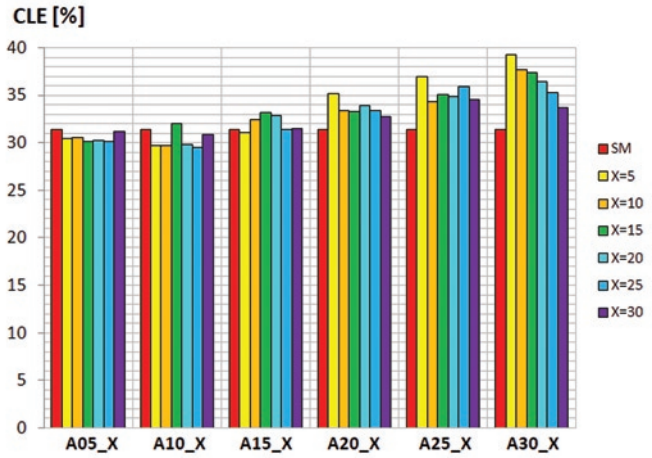

Fig. 16. Crash load efficiency in terms of relative dent depth

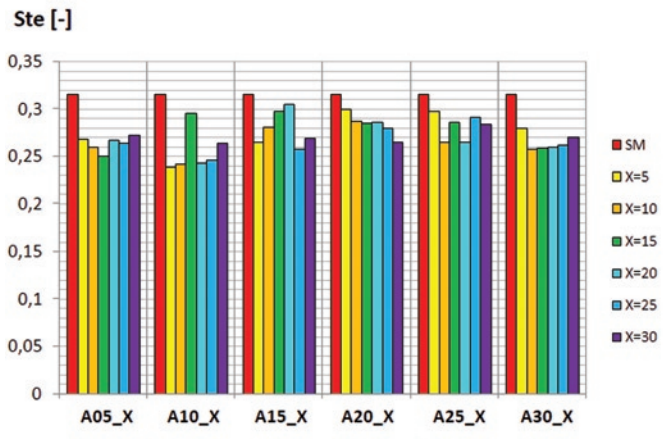

Fig. 17. Stroke efficiency in terms of relative dent depth

Fig. 15 shows a comparison of the load-shortening diagrams for columns A with the deepest dents (A30) and different X positions. These columns exhibit only the crushing mode III only.

The largest decrease of PCF was obtained for the columns with largest dent depth, which corresponds to crushing mode III and the smallest values of X (Table 3). The values of stroke efficiency (Ste) are shown in Table 4 and Fig. 17. This indicator depends on both the dent depth (A%) as well as on its position X. The smallest values are obtained for the relative dent depth (A10).

One of the most important crashworthiness indicators, both for the energy absorption capacity and for biomechanical reasons, is the CLE (mean to peak crushing force ratio). An ideal absorber should, if possible, have the CLE equal to 100%. For the columns under investigation the highest values of CLE were obtained for crushing mode III, corresponding to the deepest dents (A30) and for the smallest values of X, which is shown in Table 5 and Fig. 19. In Table 5, the shaded, grey areas visualize CLE values higher than those reperesenting the smooth column SM. The increase of the CLE in comparison with the column without dents (SM) in terms of the relative dent depth, for selected positions of X is shown in Fig. 16.

7. Conclusions

The paper reported the results of a parametric study into the energy absorption capability of thin-walled square section columns with dents. The varying parameters were the depth of the dent and the distance of the dent to the base. In addition to this, different positions of the dent,

Table 3. Peak crushing force

PCF [kN]	Column						
	SM	A05_X	A10_X	A15_X	A20_X	A25_X	A30_X
X=0	104.47	-	-	-	-	-	-
X=5	-	100.78	99.16	97.87	91.18	86.40	79.49
X=10	-	99.37	99.52	96.29	94.41	88.84	80.19
X=15	-	99.34	99.52	96.42	94.25	89.55	81.10
X=20	-	101.19	99.33	98.11	92.58	87.56	83.29
X=25	-	101.03	101.09	96.44	93.37	88.10	86.27
X=30	-	99.02	98.85	97.55	93.13	90.59	91.18

Table 4. Stroke efficiency

St_e [-]	Column						
	SM	A05_X	A10_X	A15_X	A20_X	A25_X	A30_X
X=0	0.316	-	-	-	-	-	-
X=5	-	0.268	0.239	0.265	0.300	0.298	0.280
X=10	-	0.260	0.242	0.281	0.287	0.265	0.258
X=15	-	0.250	0.296	0.298	0.285	0.286	0.259
X=20	-	0.267	0.243	0.305	0.286	0.265	0.260
X=25	-	0.264	0.246	0.258	0.280	0.291	0.262
X=30	-	0.273	0.264	0.269	0.265	0.284	0.270

Table 5. Crash load efficiency

CLE [%]	Column						
	SM	A05_X	A10_X	A15_X	A20_X	A25_X	A30_X
X=0	31.37	-	-	-	-	-	-
X=5	-	30.39	29.72	31.03	35.12	36.91	39.19
X=10	-	30.49	29.71	32.39	33.30	34.29	37.67
X=15	-	30.07	31.99	33.10	33.26	35.04	37.32
X=20	-	30.20	29.80	32.84	33.84	34.79	36.38
X=25	-	30.12	29.42	31.34	33.32	35.87	35.19
X=30	-	31.12	30.81	31.41	32.73	34.51	33.63

i.e., at the base (bottom) and at the top end (where the crushing force was applied) of the column were examined.

The results demonstrate that the main factor influencing the crushing mode and, subsequently, energy absorption capability of the column is the depth of the dent. Three crushing modes were determined. The most desirable one is that initiated (triggered) by a local plastic mechanism situated exactly at the dent. This case produced the largest values of relative dent depth (A20-A30), regardless of the position of the dent. For this crushing mode the highest values of crash load efficiency (CLE) and the smallest values of peak crushing force (PCF- Table 3) were obtained, as illustrated in Fig. 16 and Fig.19. For the deepest dents, the relative increase in the CLE amounted to about 25% for the non-flawed column. The corresponding relative decrease in the PCF amounted to about 24%. For the deepest dents, where crushing mode III could be observed, the CLE indicator decreased with elevating the dent's position. At a smaller depth of the dent, for crushing modes I and II, the dent position has little effect on the energy absorption capability of the column.

The results of the parametric study indicate that the proposed design solution of an energy absorbing thin-walled structure is efficient. Thus, further research will be conducted on multi-objective crashworthiness optimization, taking into account a wide range of geometric and material parameters. In addition to this, an experimental validation of the numerical FE model and numerical results will be performed on columns with dents using a drop hammer rig.

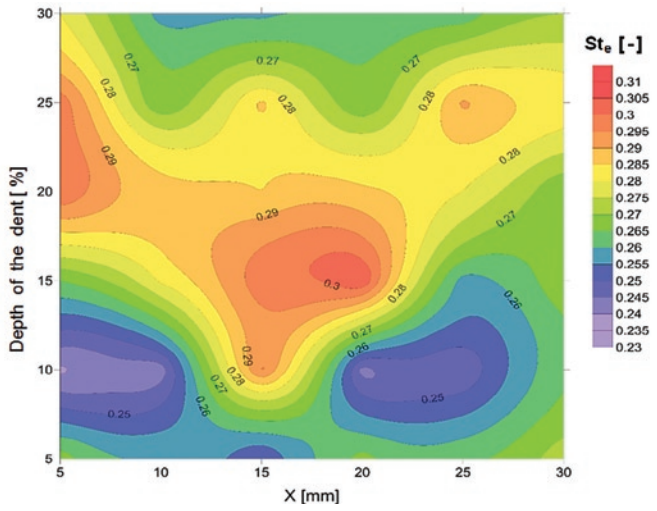

Fig. 18. Map of stroke efficiency in relative depth- position X plane

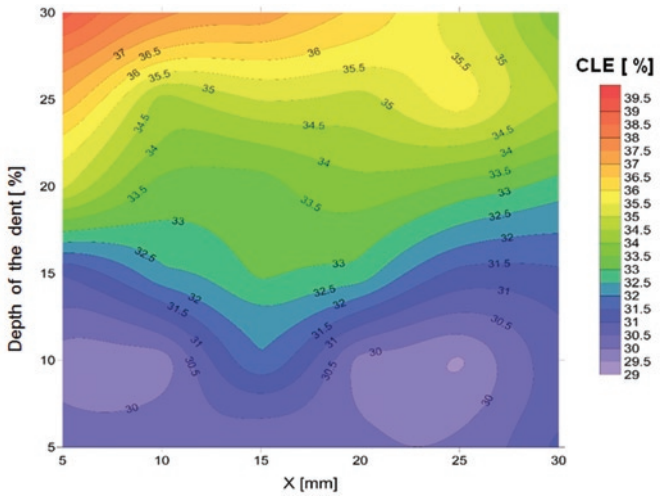

Fig. 19. Map of crash load efficiency in relative depth- position X plane

References

1. Abbasi M. et al. Multiobjective crashworthiness optimization of multi-cornered thinwalled sheet metal members, Thin Walled Struct 2015; 89: 31–41, https://doi.org/10.1016/j.tws.2014.12.009.
2. Abramowicz W. Thin-walled structures as impact energy absorbers. Thin Wall Struct. 2003; 41: 91 -109, https://doi.org/10.1016/S0263-8231(02)00082-4.
3. Alexander JM. An approximate analysis of the collapse of thin cylindrical shells under axial loading. Q J Mech Appl Math 1960; 13(1):10-15, https://doi.org/10.1093/qjmam/13.1.10.
4. Alghamdi AAA. Collapsible impact energy absorbers: an overview. Thin Wall Struct 2001; 39: 189-213, https://doi.org/10.1016/S0263-8231(00)00048-3.
5. Ali M, Ohioma E, Kraft F, Alam K. Theoretical, numerical and experimental study of dynamic axial crushing of thin walled pentagon and cross-shape tubes. Thin Wall Struct 2015; 94: 253-272, https://doi.org/10.1016/j.tws.2015.04.007.
6. Baroutaji A. et al., On the crashworthiness performance of thin-walled energy absorbers: recent advances and future developments. Thin-Walled Struct. 2017; 118: 137-163, https://doi.org/10.1016/j.tws.2017.05.018.
7. Chen W, Wierzbicki T. Relative merits of single-cell, multi-cell and foam-filled thin walled structures in energy absorption. Thin Wall Struct 2001; 39: 287-306, https://doi.org/10.1016/S0263-8231(01)00006-4.
8. Darvizeh A. et al. Low velocity impact of empty and foam filled circumferentially grooved thick-walled circular tubes. Thin Walled Struct 2017; 110: 97-105, https://doi.org/10.1016/j.tws.2016.09.002.
9. Estrada Q, Szwedowicz D, Majewski T, Martinez E, Rodriguez-Mendez A. Effect of quadrilateral discontinuity size on the energy absorption of structural steel profiles. Eksploatacja i Niezawodnosc – Maintenance and Reliability 2016; 18 (2): 186–193, https://doi.org/10.17531/ein.2016.2.5.
10. Ferdynus M. An energy absorber in the form of a thin-walled column with square crosssection and dimples. Eksploatacja i Niezawodnosc – Maintenance and Reliability 2013; 15:253-258.
11. Hanssen AG, Langseth M, Hopperstad OS. Static crushing of square aluminium extrusions with aluminium foam filler. Int J Mech Sci 1999; 41: 967-993, https://doi.org/10.1016/S0020-7403(98)00064-2.
12. Hanssen AG, Langseth M, Hopperstad OS. Static and dynamic crushing of square aluminium extrusions with aluminium foam filler. . Int J Mech Sci 2000; 24: 347-383, https://doi.org/10.1016/S0734-743X(99)00169-4.
13. Jones N. Structural Impact. Cambridge University Press 2003.
14. Jones N., Energy absorbing effectiveness factor, Int. J. of Impact Engineering 2010; 37: 754-765, https://doi.org/10.1016/j.ijimpeng.2009.01.008.
15. Kai Yang et al., Design of dimpled tubular structures for energy absorption. Thin-Walled Struct. , 2017, Thin-Walled Struct. 2017; 111: 1-8, https://doi.org/10.1016/j.tws.2016.11.004.
16. Lancaster ER, Palmer SC. Model Testing of Mechanically Damaged Pipes Containing Dents and Gouges. ASME Pressure Vessels & Piping Conference New York 1992; 235: 143–148.
17. Liu W. et al. Crushing behaviour and multi-objective optimization on the crashworthiness of sandwich structure with star-shaped tube in the center. Thin Wall Struct 2016; 108: 205-214, https://doi.org/10.1016/j.tws.2016.08.021.
18. Reddy S, Abbasi M, Fard M, Multi-cornered thin-walled sheet metal members for enhanced crashworthiness and occupant protection. Thin Walled Struct 2015; 94: 56-66, https://doi.org/10.1016/j.tws.2015.03.029.
19. Sharifi S. et al. Experimental investigation of bitubal circular energy absorbers under quasi-static axial load. Thin Wall Struct 2015; 89: 42-53, https://doi.org/10.1016/j.tws.2014.12.008.
20. Wang Q, Fan Z, Gui L. A theoretical analysis for the dynamic axial crushing behaviour of aluminium foam- filled hat sections. Int J Solids Struct 2006; 43: 2064-2075, https://doi.org/10.1016/j.ijsolstr.2005.06.011.
21. Yin H. et al. Crashworthiness optimization design for foam-filled multi-cell thin-walled structures. Thin Wall Struct 2015; 75: 8-17, https://doi.org/10.1016/j.tws.2013.10.022.
22. Zarei HR, Kroger M. Optimization of the foam-filled aluminium tube for crush box application. Thin Wall Struct 2008; 46: 214–221, https://doi.org/10.1016/j.tws.2007.07.016.
23. Zhe Yang et al. , Crushing behaviour of a thin-walled circular tube with internal gradient grooves fabricated by SLM 3D printing. Thin-Walled Struct. 2017; 111: 1-8, https://doi.org/10.1016/j.tws.2016.11.004.

Mirosław FERDYNUS
Lublin University of Technology,
Department of Machine Construction & Mechatronics,
ul. Nadbystrzycka 36, 20-618 Lublin, Poland

Maria KOTEŁKO
Lodz University of Technology,
Department of Strength of Materials
ul. Stefanowskiego 1/15 (A22), Łódź, Poland

Jan KRAL-jr
Technical University of Kosice
Faculty of Mechanical Engineering
Letna 9, 042 00 Kosice, Slovak Republic

Emails: m.ferdynus@pollub.pl, maria.kotelko@p.lodz.pl, kral.jan@tuke.sk